Available online at www.sciencedirect.com
ScienceDirect
Earth and Planetary Science Letters 248 (2006) 840–850
EPSL
www.elsevier.com/locate/epsl

Radiogenic isotopic mapping of late Cenozoic eolian and hemipelagic sediment distribution in the east-central Pacific

A.M. Stancin [a], J.D. Gleason [a,*], D.K. Rea [a], R.M. Owen [a], T.C. Moore Jr. [a], J.D. Blum [a], S.A. Hovan [b]

[a] *Department of Geological Sciences, University of Michigan, Ann Arbor, MI 48109, United States*
[b] *Department of Geological Sciences, Indiana University of Pennsylvania, Indiana, PA 15705, United States*

Received 21 February 2006; received in revised form 22 June 2006; accepted 23 June 2006
Available online 7 August 2006
Editor: S. King

Abstract

Pelagic clay of the east-central Pacific province is shown to be a mixture of three primary detrital components, reflecting continental source areas in Asia, North America, and Central and South America. Relative contributions from each source area are a function of geography, and this distribution appears to have remained constant over the past five million years, despite changing flux rates. A Q-mode factor analysis of downcore records for Pb, Sr, and Nd isotopes identified three factors that account for 98% of the total variance. These factors represent the radiogenic isotopic signatures of 1) late Cenozoic Asian dust, which dominates in the central North Pacific; 2) North American continental hemipelagic/eolian sources, restricted mainly to the easternmost North Pacific at ~30 °N latitude; and 3) Central and South American sources, restricted to areas east of ~100 °W longitude. South of the Intertropical Convergence Zone (~6 °N), the Asian dust signature diminishes abruptly. We conclude that late Cenozoic Asian dust sources can be isotopically differentiated downcore from both North American and South and Central American sources in the east-central Pacific. This approach has a utility for identifying changes in long-term Cenozoic atmospheric circulation patterns.

Keywords: Pelagic clay; North Pacific; radiogenic isotopes; Eolian Provenance; late Cenozoic

1. Introduction

Studies during the last two decades have shown that a record of past climate and atmospheric circulation can be obtained by analyzing the history of eolian dust deposition to the world oceans [1–5]. Grain size and mass flux measurements of wind-blown dust offer independent records of the changing strength of the transporting winds and the aridity of source areas, respectively [4]. Various geochemical methods have been employed to determine the sources, or provenance, of dust deposited in the oceans. Kyte et al. [6] used trace-element data on bulk samples from the giant piston core LL44-GPC3 to distinguish several source components in north central Pacific pelagic clays through the Cenozoic, including both Asian and American eolian components. Nakai et al. [7], Jones et al. [8,9] and Asahara et al. [10]

* Corresponding author.
E-mail address: jdgleaso@umich.edu (J.D. Gleason).

0012-821X/$ - see front matter © 2006 Elsevier B.V. All rights reserved.
doi:10.1016/j.epsl.2006.06.038

used radiogenic isotopes to map out variations in modern pelagic clays of the Pacific basin north of the equator. These studies, plus analyses of terrestrial deposits, including Hawaiian soil chronosequences [11] and Chinese loess deposits [9,12–14], have all identified the Central Loess Plateau of China as the dominant source of dust deposited in the present-day North Pacific.

Despite this wealth of information, there have been comparatively few downcore isotopic studies in the Pacific pelagic clay province [2]. Pettke et al. [15] tracked a 12 Myr record in a central North Pacific ODP drill site (Site 885/886) using Nd, Sr and Pb isotopes, and Ar–Ar age dating. The detrital fraction was shown to be a mixture of volcanic ash derived from the Aleutian–Kamchatka arc, and Asian dust. Significantly, they showed that the isotopic signature of the Asian-dust component did not change with time, despite an order of magnitude increase in total flux during the late Cenozoic [15]. XRD analysis has demonstrated that Pacific dust consists primarily of clay minerals (illite, with subordinate kaolinite, smectite, and chlorite) plus minor quartz and feldspar [2,15]. The illite component of Asian-derived Pacific dust has been precisely dated at ~200 Ma by Ar–Ar geochronology [15], and is another constant characteristic of this material. At site 885/886, the volcanic arc-derived ash component becomes more important with proximity to the major island arc chains of the northern and western Pacific, where the pace of volcanism has increased over the past 3 Myr [15,16]. In the South Pacific, several pelagic clay components were identified at ODP Site 596 by Zhou and Kyte [17] using geochemical data. They interpreted these components as detrital (non-Asian eolian), andesitic (volcanic), hydrothermal, hydrogenous, phosphatic (fish debris) and biogenic silica, though no radiogenic isotope data have been obtained on the detrital component.

A more recent study by Hyeong et al. [18] on a 3 m piston core from the northeast equatorial Pacific detected mineralogical and geochemical changes at the 2.5 m depth, which they attributed to a shift in sources for the eolian component. They interpreted this to represent a late Miocene southward shift in the latitude of the Intertropical Convergence Zone (ITCZ), which they concluded had been north of the core site (~12 °N) prior to the late Miocene. Hovan [5] reported similar findings based on grain size analysis of ODP leg 138 cores in the equatorial East Pacific. As presently understood, the ITCZ (synonymous with the low pressure equatorial trough) forms an effective rain barrier to dust transport between the hemispheres [4]. This is observed in the present-day distribution of Asian dust that extends south to the ITCZ at approximately 6 °N (modern annual average in the Pacific region), as mapped by Nd isotopes [8], and in the order of magnitude drop in eolian mass accumulation rate from north to south across the ITCZ [4]. Downcore radiogenic isotopic studies of core LL44-GPC3 have identified a possible shift in the ITCZ of >20° latitude in the central Pacific between 30 and 40 Ma [4,19]. The ODP leg 199 work of Lyle et al. [20] supports this finding, as recorded by a shift from smectite to illite dominated mineralogy in the equatorial central Pacific around this time. The downcore change from illite to smectite was also noted by Griffen and Goldberg [21]. More recent work (Gleason unpublished data; [22]) has placed this apparent isotopic transition closer to the Eocene–Oligocene boundary.

Here, we present new Pb, Sr, and Nd isotope ratio measurements for the 0–5 Ma extracted detrital mineral component (<38 μm) over a portion of the eastern and central Pacific. Included are continental margin hemipelagic samples from offshore North America, Central America, and South America, in addition to samples from the central North Pacific pelagic clay province [2]. Samples were obtained from the Deep Sea Drilling Project (DSDP), the Ocean Drilling Program (ODP), and piston cores recovered by the R/V Ewing (EW9709). The data were combined with several other complete Nd, Sr and Pb isotope data sets and analyzed using factor analysis to address the following questions: 1) can we differentiate quantitatively between North American and South/Central American sediment sources in the Pacific? 2) what was the stability of the Asian–American Dust Boundary (AADB) over the last 5 Myr? 3) what are the geographical limits of Asian dust influence through time? 4) can this approach be used to track the position of ITCZ through time?

2. Methods and procedures

All samples were processed by reductive cleaning following the methods of Rea and Janecek [23] and Hovan [5] for complete removal of biogenic opal, calcium carbonate, and authigenic Fe–Mn oxyhydroxides. Samples of the sub-63 micron detrital extract were further processed by sieving to isolate the sub-38 micron fraction, followed by additional cleaning with 1 M ammonium acetate [15].

After freeze-drying, approximately 40 mg of material from each sample was digested for Nd, Sr and Pb isotopic analysis using a combination of HF–HNO_3, $HClO_4$ and HCl in screw-top teflon beakers. Two overnight hotplate digestions at 120 °C in concentrated HF–HNO_3 (5:1 ratio) were employed to break down silicates, followed by a capped overnight digestion in concentrated HNO_3 to help drive off fluorides and oxidize organics. Perchloric acid digestion at 160 °C destroyed any remaining organics

and fluorides, resulting in completely clear solutions when redissolved in HCl. The rare earth element (REE) fraction and Sr were separated from the matrix by conventional cation exchange chromatography using 10 cm quartz glass columns packed with AG 50W-X8 cation exchange resin pre-conditioned with 2 M HCl. Strontium was eluted with 2 M HCl, and REE were eluted in 6 M HCl. The REE fraction was treated with $HClO_4$ to drive off remaining organics, and loaded on HDEHP-teflon columns in 0.22 N HCl for separation of Nd by reverse phase chromatography [24]. Strontium was processed through a second separation stage on miniaturized columns packed with strontium-specific (Sr-Spec) crown ether resin to further purify Sr.

The Nd and Sr isotopic ratios were determined at the University of Michigan on a Finnigan 262 solid source thermal ionization mass spectrometer equipped with 8 collectors; Nd was loaded on rhenium filaments as a chloride, with a second filament used to ionize Nd. Nd was measured in static mode as the Nd+ ion. Data were collected on 150 ratios with a beam intensity of 1.7 V on mass 142, yielding typical uncertainties of $<0.0015\%$ in the $^{143}Nd/^{144}Nd$ ratio. Mass 147 was monitored to insure no Sm interference on mass 144. The $^{143}Nd/^{144}Nd$ ratios were normalized to $^{146}Nd/^{144}Nd=0.7219$ using an online exponential law fractionation correction. The La Jolla Nd standard gave a mean value of $^{143}Nd/^{144}Nd=0.511849\pm0.000012$ ($N=27$) over the course of this study. External

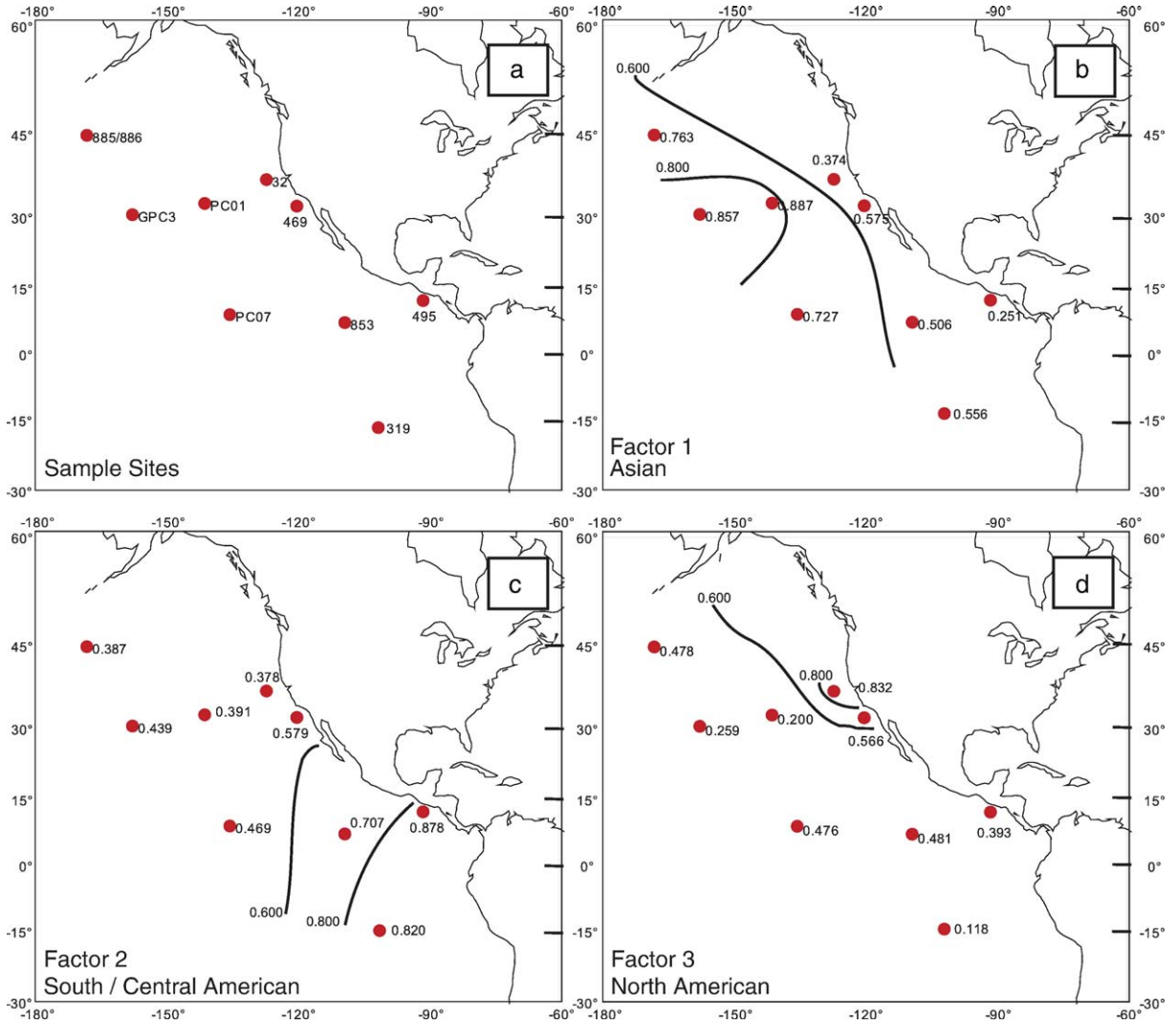

Fig. 1. a–d. Site and contour maps showing average Q-factor values from Varimax factor loadings of Nd, Sr and Pb isotopic composition data (Table 2 and supplemental table) for the eastern Pacific, computed with the program CABFAC (see text). The Asian dust signature (1b) dominates the central North Pacific, while South/Central American (1c) and North American (1d) sources dominate closer to continental margins.

reproducibility of ε_{Nd}, based on several replicate digests of the same sample, is estimated at ±0.25 epsilon units, where $\varepsilon_{Nd}=10^4[(^{143}Nd/^{144}Nd_{(t)SAMPLE})/(^{143}Nd/^{144}Nd_{(t)CHUR})-1]$; $^{143}Nd/^{144}Nd_{(t)CHUR}=0.512638$ (Bulk Earth). Strontium was loaded as a chloride on a single W filament with tantalum oxide powder and phosphoric acid. Data were collected by static mode analysis on 150 ratios with beam strength of ~2.5 V on mass 88, yielding typical uncertainties of <0.0020% in the $^{87}Sr/^{86}Sr$ ratio. Mass 85 was monitored to insure minimum Rb interference on mass 87. The $^{87}Sr/^{86}Sr$ ratios were normalized online to $^{86}Sr/^{88}Sr=0.1194$; Sr standard NBS 987 yielded a mean value of $^{87}Sr/^{86}Sr=0.710250\pm0.000014$ ($N=74$). Total procedure Sr and Nd blanks were typically ~100 and ~50 pg, respectively, equivalent to <1/1000 of the typical sample processed, thus requiring no correction.

Pb separation was carried out following the methods of Reuer et al. [25]. Miniaturized anion exchange columns were packed with AG1-X8 200–400mesh anion-exchange resin and pre-conditioned in 1 M HBr. Samples were loaded in 1 M HBr and eluted with 2 M HCl and 6 M HCl. Recovery of Pb was >99% in the 1 ml 6 M HCl fraction. Pb isotopic compositions were measured on a Nu Instrument multi-collector ICP-MS at the University of Michigan using a standard-sample-standard bracketing technique and thallium internal normalization [25,26]. All analyses were conducted in static mode utilizing a 7 faraday collector array for masses 202 through 208. Samples were aspirated in 5% HNO_3 using an Aridus desolvating nebulizer. Data were collected in 2 blocks of 15 ratios each. 3 V signals were typically obtained on mass 208 for ~50 ppb Pb solutions under normal operating conditions. Hg was always below detection limits during Pb analysis, hence no correction was necessary. Blank levels were monitored at all stages of the procedure, and were usually less than 1/1000 of total Pb analyzed.

Normalization of Pb isotopic data to SRM-981 [27], yielded highly reproducible data under standard operating conditions. 1-sigma precision on individual $^{207}Pb/^{206}Pb$ and $^{208}Pb/^{206}Pb$ ratios was typically ±0.002% collected on 30 ratios, with precision (true within-run reproducibility) approximately a factor of two greater (±0.005%) based on >100 runs of the NBS-981 Pb isotope standard. Precision on $^{206}Pb/^{204}Pb$, $^{207}Pb/^{204}Pb$, and $^{208}Pb/^{204}Pb$ ratios averaged ±0.01% on 30 ratios with approximately a factor of two higher reproducibility (±0.02%) based on >100 runs of the NBS-981 Pb isotope standard. Duplicate digest analyses of samples, and of the SRM-981 standard (run as an unknown), indicate our true reproducibility (2-sigma) is $^{206}Pb/^{204}Pb=\pm0.013\%$, $^{207}Pb/^{204}Pb=\pm0.008\%$, $^{208}Pb/^{204}Pb=\pm0.010\%$, $^{207}Pb/^{206}Pb=\pm0.004\%$ and $^{208}Pb/^{206}Pb=\pm0.006\%$. The reproducibility (2-sigma) of the SRM981 Pb standard is: $^{208}Pb/^{204}Pb=36.6656+/-0.0029$, $^{207}Pb/^{204}Pb=15.4820+/-0.0011$, $^{206}Pb/^{204}Pb=16.9307+/-0.0012$, $^{208}Pb/^{206}Pb=2.16562+/-0.00006$ and $^{207}Pb/^{206}Pb=0.91443+/-0.00002$. Procedural blanks for the period of analysis ranged from 100 to 500 pg. The Pb blank levels are estimated at between 0.2% and 0.1% of the total sample and no blank corrections were performed.

3. Factor analysis

Factor analysis has been applied in the geosciences, most commonly in paleontological studies, but also to geochemical and mineralogical data sets, and in particular to the geochemistry of marine sediments [6,28–30]. Q-mode factor analysis reduces a matrix of data to a few factors that explain a stated portion of the variance in the data set. In this study, the Varimax rotated matrix mathematically defines three factors which explain 98.6% of the variance in the data. The data from each sample can then be expressed in terms of contributions from each factor (factor loadings). For example, at site PC-01, there is a 0.887 contribution from factor 1, 0.391 of factor 2, and 0.2 from factor 3 (Fig. 1). The higher the factor loading, the greater the influence a factor has on a given sample. The sum of the squares of the factor loadings for each sample (the

Table 1
Factor loadings and communality for radiogenic isotopic data from Pacific deep sea cores (0–5 Ma)

	Factor 1	Factor 2	Factor 3	Square of factor 1	Square of factor 2	Square of factor 3	Communality
PC-01	0.887	0.391	0.2	0.787	0.153	0.040	0.980
PC-07	0.727	0.469	0.476	0.529	0.220	0.227	0.975
885/886	0.763	0.387	0.478	0.582	0.150	0.228	0.960
GPC-3	0.857	0.439	0.259	0.734	0.193	0.067	0.994
32	0.374	0.378	0.832	0.140	0.143	0.692	0.975
469	0.575	0.579	0.566	0.331	0.335	0.320	0.986
853	0.506	0.707	0.481	0.256	0.500	0.231	0.987
495	0.251	0.878	0.393	0.063	0.771	0.154	0.988
319	0.556	0.82	0.118	0.309	0.672	0.014	0.995

Table 2
New Nd–Sr–Pb isotope data generated for this study (detrital extract <38 μm) from Pacific deep sea cores (0–5 Ma)

Core	Leg/site/core/section/interval (cm)/depth (mbsf)	Age (Ma)[a]	$^{143}Nd/^{144}Nd$	ε_{Nd}	$^{87}Sr/^{86}Sr$	$^{208}Pb/^{204}Pb$	$^{207}Pb/^{204}Pb$	$^{206}Pb/^{204}Pb$	$^{208}Pb/^{206}Pb$	$^{207}Pb/^{206}Pb$	μ	κ
ODP site 853	138/853B/2H-2/60–64/6.4	1.5	0.512304	−6.5	0.706800	38.6993	15.6195	18.8406	2.053929	0.892904	9.27	3.93
ODP site 853	138/853B/2H-4/60–64/9.4	2.1	0.512290	−6.8	0.707905	38.8430	15.6353	18.9416	2.050391	0.825358	9.37	3.95
ODP site 853	138/853B/3H-1/55–60/12.9	3.4	0.512436	−3.9	0.705415	38.5470	15.6014	18.7827	2.052096	0.830601	9.21	3.89
ODP site 853	138/853B/4H-2/55–60/22.4	3.9	0.512408	−4.5	0.705733	38.5160	15.6007	18.7555	2.053391	0.831770	9.19	3.89
EW9709-01	0.0 mbsf	0	0.512114	−10.2	0.725353	38.9307	15.6533	18.8429	2.066010	0.830750	9.27	4.03
EW9709-01	1.50 mbsf	5	0.512156	−9.4	0.723842	38.9346	15.6578	18.8331	2.067308	0.831462	9.26	4.04
EW9709-07	0.0 mbsf	0	0.512110	−10.3	0.718722	39.0151	15.6629	18.9888	2.054582	0.824894	9.41	4.00
EW9709-07	1.50 mbsf	5	0.512152	−9.5	0.711519	38.8014	15.6411	18.8506	2.058266	0.829719	9.28	3.97
ODP site 495	67/495/9/5/37–40/82.37	2	0.512841	4	0.704827	38.5325	15.6012	18.7535	2.054640	0.831890	9.20	3.91
ODP site 495	duplicate (dry splits, independently processed)	2	0.512839	3.9	0.704792	38.5308	15.5983	18.7501	2.054675	0.831914	9.18	3.90
ODP site 495	67/495/13/3/30–33/117.30	5	0.512873	4.6	0.705063	38.5847	15.6005	18.8076	2.051521	0.829434	9.24	3.90
ODP site 495	67/495/13/2/40–43/115.90	5	0.512787	2.9	0.704549	38.5300	15.6229	18.7504	2.058175	0.834528	9.15	3.91
ODP site 469	63/469/7/1/50–53/55.5	2	0.512222	−8.1	0.709948	38.8619	15.6421	18.9092	2.055311	0.827020	9.33	3.97
ODP site 469	duplicate (dry splits, independently processed)	2	0.512204	−8.5	0.709903							
ODP site 469	63/469/11/3/72–75/96.72	5	0.512253	−7.5	0.708823	38.7498	15.6510	18.9740	2.042225	0.824868	9.40	3.90
ODP site 469	63/469/12/1/72–75/103.22	5	0.512276	−7.1	0.708559	38.9004	15.6404	18.9235	2.055611	0.826604	9.35	3.98
ODP site 319	34/319/1/3/120–123/4.49	5	0.512288	−6.8	0.707553	38.2993	15.5699	18.5102	2.069080	0.841137	8.95	3.90
ODP site 319	duplicate (dry splits, independently processed)	5	0.512298	−6.6	0.707485	38.2933	15.5686	18.5086	2.068957	0.841147	8.95	3.89
ODP site 319	34/319/1/6/110–113/8.89	5	0.512275	−7.1	0.707670	38.2288	15.5574	18.4806	2.068572	0.841788	8.92	3.88
ODP site 319	34/319/1/4/108–111/5.87	5	0.512282	−6.9	0.707601	38.2844	15.5678	18.5089	2.068413	0.841087	8.95	3.89
ODP site 319	34/319/2/3/106–111/13.56	5	0.512256	−7.5	0.708447	38.0987	15.5405	18.4211	2.068215	0.843592	8.86	3.85
ODP site 319	34/319/1/5/106–110/7.35	5			0.707431	38.1466	15.5531	18.4122	2.071767	0.844682	8.85	3.87
ODP site 32	5/32/3/2/4–7/81.81	2	0.512323	−6.1	0.708522	39.0384	15.6751	19.1865	2.034631	0.816962	9.60	3.92
ODP site 32	5/32/3/5/5–9/86.32	5	0.512363	−5.4	0.707452	39.0693	15.6731	19.2648	2.027943	0.813548	9.60	3.93

[a] Ages revised using time-scale of Berggren et al. [47].

communality of the sample) indicates how well each sample is explained by the factor solution. This communality should approach one (Table 1); the communality of the sample PC-01 is 0.98. For this study, a matrix of variables, consisting of $^{208}Pb/^{204}Pb$, $^{207}Pb/^{204}Pb$, $^{206}Pb/^{204}Pb$, $^{208}Pb/^{206}Pb$, $^{207}Pb/^{204}Pb$, ε_{Nd}, $^{87}Sr/^{86}Sr$, and the calculated Pb model isotopic values of μ and κ (Table 2 and supplemental table) was

processed by Q-mode factor analysis using the program CABFAC [31]. Values were normalized to values of 0–1 using the range of each variable [32].

The time integrated $^{238}U/^{204}Pb$ ratio of the source is referred to as μ and κ is the time-integrated $^{232}Th/^{238}U$ of the source, calculated from the Pb isotopic ratios. These parameters were calculated using the single stage Holmes–Houtermans model, and the initial bulk earth Pb isotopic values of Tatsumoto [33], where

$$\mu = \frac{\left(\frac{^{206}Pb}{^{204}Pb}\right)_t - \left(\frac{^{206}Pb}{^{204}Pb}\right)_i}{e^{\lambda_1 T} - e^{\lambda_1 t}} = \frac{^{238}U}{^{204}Pb}\,(\text{source reservoir})$$

and

$$\kappa = \frac{\omega}{\mu}$$

Where

$$\omega = \frac{\left(\frac{^{208}Pb}{^{206}Pb}\right)_t - \left(\frac{^{208}Pb}{^{206}Pb}\right)_i}{e^{\lambda_3 T} - e^{\lambda_3 t}} = \frac{^{232}Th}{^{204}Pb}\,(\text{source reservoir})$$

4. Results and discussion

In this rather small sample set, factor 1, which accounts for 43.1% of the total variance (Table 3), represents the isotopic signature of Asian-derived dust that dominates surface sediments in the central North Pacific pelagic clay province [7,8,4]. The isotopic component most definitive of the Asian signature is ε_{Nd} (Table 3). Factor 2 accounts for 34.3% of the total variance, and defines a South and Central American geochemical signature that is likely a combination of both eolian and hemipelagic (or "andesitic") components [4]. The principle components defining a South and Central American provenance signature are $^{208}Pb/^{204}Pb$, $^{207}Pb/^{204}Pb$, $^{206}Pb/^{204}Pb$, and μ (Table 3). Factor 3 accounts for 21.2% of the variance, and defines a North American "shale" signature that is also likely both hemipelagic and eolian in origin [4]. The principle components identified by factor analysis for the North American signature are $^{208}Pb/^{206}Pb$, $^{207}Pb/^{206}Pb$ and κ (Table 3).

Table 3
Results of factor analysis using Nd–Sr–Pb isotope ratios in Pacific deep marine cores (0–5 Ma)

Factor	Percent of variance	Key component
Factor 1 Asian	43%	ε_{Nd}
Factor 2 South/ Central American	34%	$^{208}Pb/^{204}Pb$ $^{207}Pb/^{204}Pb$ $^{206}Pb/^{204}Pb$ μ
Factor 3 North American	21%	$^{208}Pb/^{206}Pb$ $^{207}Pb/^{206}Pb$ κ

Computed from Table 1 and supplemental online file.

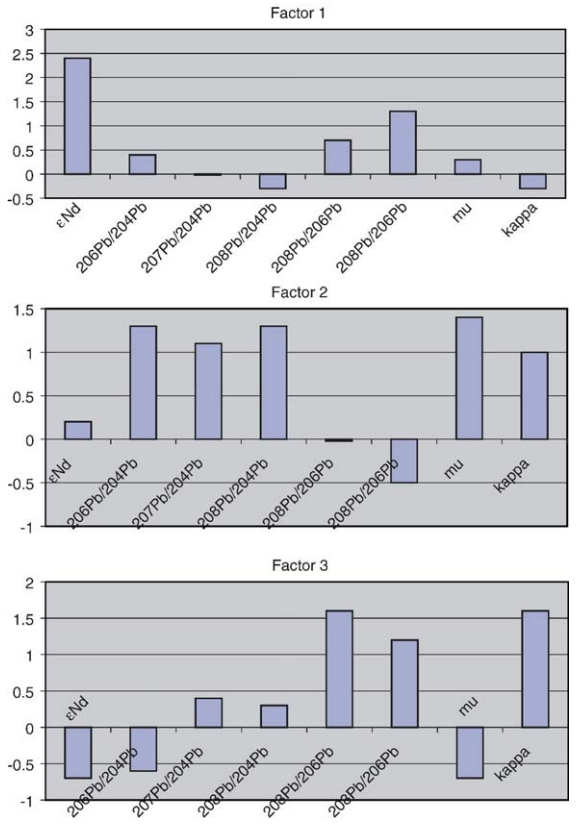

Fig. 2. Factor scores for each variable in the end-member variance identified by factor analysis [46] using CABFAC [28]. In each of these plots, larger numbers indicate larger contributions.

Plotting and contouring the Varimax rotated factor loadings shows how the distribution of these three distinct signatures has varied in the eastern central Pacific over the last 5 Myr. (Fig. 1b, c, d). The most northern site (ODP 885/886, Fig. 1) exhibits a slightly lower factor 1 contribution, due to the presence of volcanic ash in some of the core samples [15,16]. The South/Central American signature is primarily defined by the southern hemisphere ODP Site 319, west of Peru. North American sources are defined by DSDP Site 32 off northern California, and to a lesser extent Site 469, located off the California coast. Piston cores LL44-GPC3, EW9709-01 and EW9709-07, along with ODP Site 885/886 in the central North Pacific, help define the limits of the Asian dust influence (see maps of Jones et al. [8,9]). ODP Sites 853 and 495 are more under the influence of Central American volcanic and hemipelagic sources, respectively. The factor scores of the variables are plotted in Fig. 2 to

demonstrate the relative importance of each end member. In this figure, larger numbers (absolute values) indicate larger contributions.

For comparison with the above results, isotopic contour maps were also produced (Fig. 3a–g) for surface sediment Nd, Sr and Pb compositions in the Pacific, using a larger data set. The geographical pattern for Nd isotopes (Fig. 3a) most clearly shows the limits of present-day Asian dust influence, as originally mapped by Nakai et al. [7] and Jones et al. [8]. Sites near volcanic regions have more positive values, while most of the central North Pacific pelagic clay province shows the Asian dust source Nd isotopic signature of −10, which is virtually invariant [7,8,15,34]. Near continental margins, the eolian component is clearly overwhelmed by the approximately 2–3 orders of magnitude greater flux of hemipelagic sediment [4,9].

Our new data implies that the overall isotopic pattern in the Pacific has been relatively stable over the last ~5 Myr. Strontium isotopic data for the Pacific region (Fig. 3b) are taken largely from the detailed data sets of Asahara et al. [10,35] and Nakai et al. [7]. Sr isotopes track Nd fairly closely, but as observed elsewhere [10,36–39], finer-grained pelagic clay fractions tend to have more radiogenic strontium than coarser-grained fractions. Therefore, some of the detail in Fig. 3b could be in part an artifact of unmixing and grain size effects within the smallest dust clay size fraction. The highest values of $^{87}Sr/^{86}Sr$ are found in the north central Pacific away from the influence of arc volcanism and hemipelagic sedimentation, as with unradiogenic Nd. Though quite variable in its source region, Asian loess that is deposited in the central North Pacific has a fairly constant $^{87}Sr/^{86}Sr$ of approximately 0.720 [10,14]. Because it has been found that the more radiogenic Sr is concentrated in smaller grain size fractions within individual samples [10], the regional pattern could reflect a similar sorting process. However, as reported by Rea and Hovan [40], particle size ceases to vary in a systematic way many 1000's of km down-plume in the central North Pacific. Thus, the close match between the isotopic, grain size and grain-sorting patterns of central North Pacific pelagic clays most likely reflects the near 100% dominance of Asian-derived dust over other sources in this part of the Pacific [40].

The Pb isotope contour maps (Fig. 3c–g) broadly reinforce the Nd–Sr contour maps with the following exceptions:

1) An area of low $^{207}Pb/^{206}Pb$ and $^{208}Pb/^{206}Pb$ is defined off the coast of N. America, and
2) The pattern established by the other isotopic signatures is much more poorly defined for $^{206}Pb/^{204}Pb$

The unusual $^{206}Pb/^{204}Pb$ signature is perhaps due in part to volcanic ash produced by North Pacific island arcs, or to sediment derived from erosion of these island arcs. Pettke et al. [15] found that volcanic ash is a significant component in the North Pacific, and may have influenced the $^{206}Pb/^{204}Pb$ ratio more than other ratios. In general, however, the regional isotopic variations that Jones et al. [8,9] defined on the basis of Nd and Pb isotopes are reinforced by our contour mapping.

The combined Nd, Sr and Pb isotope data are suggestive of plumes of isotopically distinct dust coming off the Asian deserts and traveling across the Pacific to North America [9]. This material is presently transported 1000's of km from its source, usually as spring dust storms [4]. The Asian dust signature is lost in the marine record near North America because of the dramatically higher flux of hemipelagic material near the continental margins [41]. We note, as did Jones et al. [9], that Sr and Nd isotope signatures are much more distinct than those of Pb for distinguishing Pacific volcanic arc sources from Asian loess. However, computed κ values (time-averaged Th/U ratios) suggest that the source reservoir of the Asian loess has a time-averaged Th/U ratio distinct from other sources of central North Pacific sediment. As with Sr isotopes, there may be a tendency in the U, Th and Pb system to be influenced by grain size effects which vary as a function of proximity to source areas, though to our knowledge such effects have not been studied directly. Another possibility for the less coherent patterns in the Pb isotopes is that volcanic Pb adsorbing onto clay particles may also be partly masking the eolian Pb signature in the North Pacific [19]. Adding to this, Van de Flierdt et al. [41] suggested that erosion of young volcanics was a major source of dissolved Pb in the Pacific Ocean. This would suggest that Pb isotopes, at least in the volcanically active North Pacific, may not be as reliable an indicator of provenance of the detrital fraction, despite the employment of careful cleaning procedures for samples (see Methods and procedures) in this study.

Isotope variation plots show the geochemical trends in the Pacific data set (Fig. 3a–b). Fig. 4a (ε_{Nd}-Sr isotope plot) shows that central North Pacific sites are generally all within one standard deviation of the ε_{Nd} value of −10 (+/−0.4), reflecting the Asian Nd component [8]. Points that were not clearly grouped within the Asian dust regime were all from Site 885/886 [15] and appear to be influenced by the Kamchatka Arc system. Site 495, adjacent to the Central American arc is characterized by highly radiogenic Nd (ε_{Nd}=5) and forms a distinct group. On this plot, North and South/Central American overlap.

The North and South/Central American components are distinguished more readily on the Pb isotope plots (Fig. 4b).

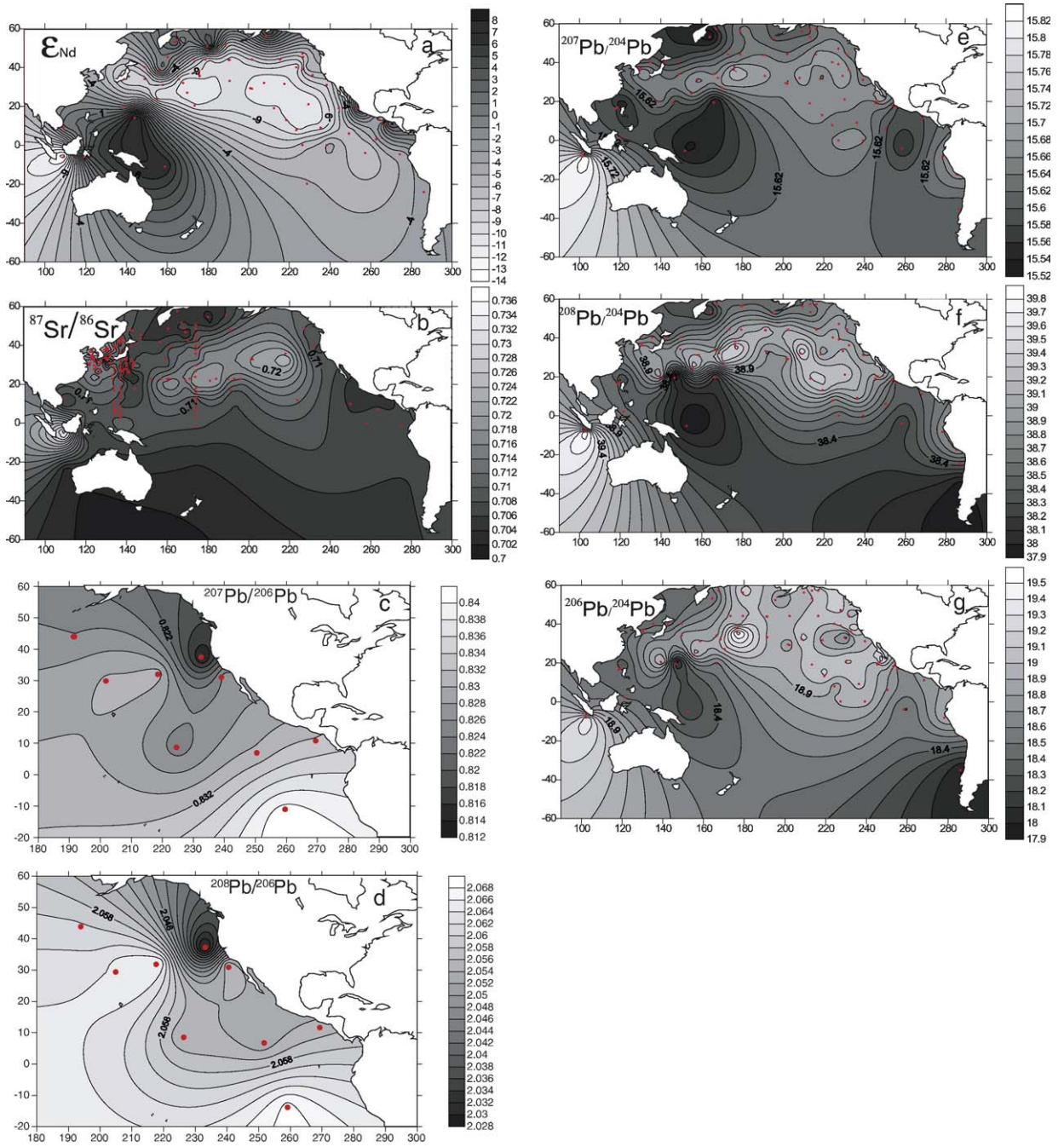

Fig. 3. a–g. Contour maps of Nd, Sr and Pb isotopic values of the extracted terrigenous component in Pacific Ocean surface sediments 0–5 Ma. The Asian Nd isotopic signature (3a) dominates a large region within the central North Pacific pelagic clay province. The most radiogenic $^{87}Sr/^{86}Sr$ values (3b) appear to be focused towards the center of the North Pacific gyre, significantly downwind from Asian dust sources. The components identified by factor analysis as defining a North American source were $^{207}Pb/^{206}Pb$ (3c) and $^{208}Pb/^{206}Pb$ (3d). Both clearly show minimum values just off the coast of California. $^{207}Pb/^{204}Pb$ (3e) and $^{208}Pb/^{204}Pb$ (3f) both reveal the Asian dust plume as defined by Jones et al. [9]. The $^{206}Pb/^{204}Pb$ ratio (3g) does not (see text). Data are from this paper, McLennan et al. [43], Nakai et al. [7], Asahara et al. [10,35], Jones et al. [9], Pettke et al. [15,19] and Hemming et al. [44]. Areas with a higher density of data points yield contours with a higher degree of confidence than areas with few or no data points. The plots were produced using *PanMap* [45] and Surfer 7.0.

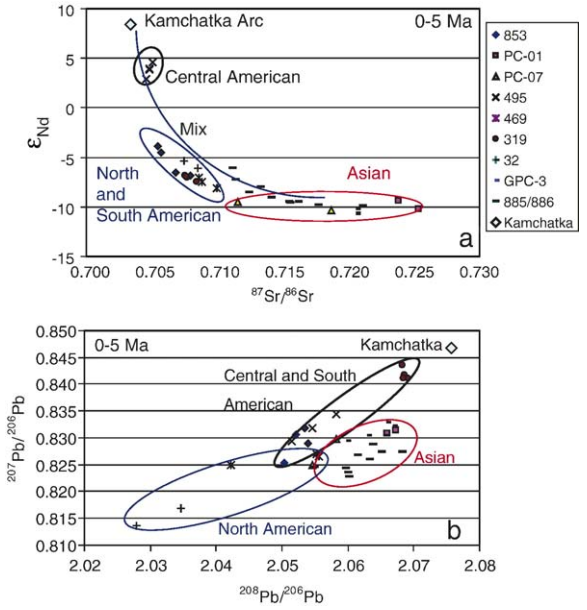

Fig. 4. a–b. In (4a), the Asian dust signature appears as a discrete component with $\varepsilon_{Nd}=-10$ and radiogenic $^{87}Sr/^{86}Sr$ values (0.715 to 0.725). Site 885/886 is located nearer the Kamchatka volcanic arc region and shows mixing with a more juvenile volcanic arc component [15], while ODP Site 495 off Central America is also characterized by more mantle-like values, implying young volcanic sources. (4b) shows the distinctive South American and North American Pb isotopic signatures. The Kamchatka Arc point was an average from the GEOROC geochemical data base (http://georoc.mpch-mainz.gwdg.de/georoc). All data from this study except Site 885/886 [15] and LL44-GPC3 [7,19].

The North American component is distinguished by lower $^{207}Pb/^{206}Pb$ and $^{208}Pb/^{206}Pb$ (Fig. 4b). Approximate isotopic end members were also calculated for each grouping (Table 4). The end member compositions calculated for each component are highlighted. Pettke et al. [15] determined Pb isotopic end members for the non-anthropogenic Asian loess component as $^{206}Pb/^{204}Pb=18.97+/-0.06$, $^{207}Pb/^{204}Pb=15.67+/-0.02$ and $^{208}Pb/^{204}Pb=39.19+/-0.11$, which are very similar to our Asian Pb isotopic end members. These values, along with an $\varepsilon_{Nd}=-10.2+/-0.5$, isotopically define the Asian dust end member.

In summary, contour plots of the factor analysis results, coupled with surface sediment contour plotting and plots of Nd, Sr and Pb isotope ratios, support highly stable and well-established North Pacific atmospheric circulation patterns over the last 5 Myr, as the northern hemisphere cooled towards ice age conditions. This should not be surprising, as intense desertification of the Asian interior is well-documented for the period prior to 2.6 Ma, when an order of magnitude increase in dust delivery to the central North Pacific commenced [4,42]. The ITCZ is a clear demarcation line for Asia-derived dust [4,8,9,15,19] between the northern and southern hemispheres over the last 5 Myr, and probably much earlier [4,15,19]. We find that not only is the geochemical signature of Asian dust quantitatively distinct from both North American and South American signatures, but there is a difference between the American sources as well, reinforcing the efficacy of employing multiple isotopic systems for regional provenance studies. Extending this type of analysis to additional sites within the Pacific basin promises to reveal in considerably more detail how atmospheric circulation may have varied as a function of Cenozoic climate change.

Table 4
Sr–Nd–Pb radiogenic isotopic end members computed for Pacific deep sea cores (0–5 Ma)

		$^{143}Nd/^{144}Nd$	ε_{Nd}	$^{87}Sr/^{86}Sr$	$^{208}Pb/^{204}Pb$	$^{207}Pb/^{204}Pb$	$^{206}Pb/^{204}Pb$	$^{208}Pb/^{206}Pb$	$^{207}Pb/^{206}Pb$	μ	κ
Asian $n=19$	average	0.51213	−9.44	0.7174	39.02	15.66	18.92	2.062	0.828	9.3	4.04
	S.D.	0.00002	1.22	0.0044	0.15	0.02	0.08	0.004	0.003	0.1	0.04
Asian w/o 885/886	average	0.51213	−10.22	0.7203	38.91	15.66	18.86	2.063	0.830	9.3	4.01
volcanic component $n=9$	S.D.	0.00002	0.50	0.0038	0.06	0.01	0.06	0.005	0.002	0.1	0.02
Central American	average	0.51260	−0.79	0.7056	38.60	15.61	18.79	2.054	0.831	9.2	3.91
$n=8$	S.D.	0.00026	5.07	0.0012	0.12	0.01	0.07	0.002	0.003	0.1	0.02
Central American	average	0.51284	3.85	0.7048	38.54	15.61	18.76	2.055	0.832	9.2	3.90
w/o 853 $n=4$	S.D.	0.00004	0.70	0.0002	0.03	0.01	0.04	0.003	0.002	0.0	0.01
North American	average	0.51229	−6.84	0.7087	38.92	15.66	19.05	2.043	0.822	9.5	3.94
$n=5$	S.D.	0.00006	1.09	0.0009	0.13	0.02	0.16	0.012	0.006	0.1	0.04
South American	average	0.51232	−6.25	0.7071	38.44	15.59	18.66	2.061	0.836	9.1	3.90
$n=10$	S.D.	0.27388	1.31	0.0011	0.25	0.03	0.20	0.009	0.007	0.2	0.03
South American	average	0.51228	−7.08	0.7078	38.23	15.56	18.48	2.069	0.842	8.9	3.88
w/o 853 $n=6$	S.D.	0.00001	0.31	0.0004	0.09	0.01	0.04	0.000	0.001	0.0	0.02

Computed from Table 1 and online supplemental file.

5. Conclusions

Q-mode factor analysis of data from marine cores suggests three distinct provenance groupings in the east-central Pacific identified by their Sr, Nd and Pb isotopic composition. These three factors account for 98.7 percent of the variance. Factor 1 (43% of the total variance) is defined most strongly by ε_{Nd} and is associated with Asian-derived dust. Factor 2 (34% of the total variance) is defined mainly by $^{208}Pb/^{204}Pb$, $^{207}Pb/^{204}Pb$, $^{206}Pb/^{204}Pb$ and μ and is associated with South and Central American sources. Factor 3 (21% of the total variance) is dominated by $^{208}Pb/^{206}Pb$, $^{207}Pb/^{206}Pb$ and κ and defines a distinct North American source. We conclude that late Cenozoic Asian dust sources can be clearly differentiated from American continental sources, and that North and South/Central American sources can also be distinguished from each other.

Acknowledgments

We thank B. Klaue, A. Klaue and M. Johnson for laboratory assistance. Samples were provided by the DSDP/ODP core repositories at the Scripps Institution of Oceanography and Texas A&M University, and by the Core Laboratory of the College of Oceanic and Atmospheric Science at Oregon State University. This research was funded by NSF grant #OCE-0136829. We appreciate the reviews of Thomas Pettke and two anonymous reviewers, which greatly improved this paper.

Appendix A. Supplementary data

Supplementary data associated with this article can be found, in the online version, at doi:10.1016/j.epsl.2006.06.038.

References

[1] T.R. Janecek, D.K. Rea, Eolian deposition in the northeast Pacific Ocean: Cenozoic history of atmospheric circulation, Geol. Soc. Amer. Bull. 94 (1983) 730–738.
[2] M. Leinen, The pelagic clay province of the north Pacific Ocean: the geology of North America, v. N: the eastern Pacific Ocean and Hawaii, Geol. Soc. Amer. (1989) 323–335.
[3] A.M. Olivarez, R.M. Owen, D.K. Rea, Geochemistry of eolian dust in Pacific Ocean sediments: implications for paleomagnetic interpretations and the REE budget of seawater, Geochim. Cosmochim. Acta 92 (1991) 2147–2158.
[4] D.K. Rea, The paleoclimatic record provided by eolian deposition in the deep sea, the geologic history of wind, Rev. Geophys. 32 (1994) 159–195.
[5] S.A. Hovan, Late Cenozoic atmospheric circulation intensity and climatic history recorded by eolian deposition in the eastern equatorial Pacific, leg 138, in: N.G. Pisias, L.A. Mayer, et al., (Eds.), Proceedings of the Ocean Drilling Program, Texas A&M University, Scientific Results, College Station, Texas, vol. 138, 1995, pp. 615–625.
[6] F.T. Kyte, M. Leinen, G.R. Heath, L. Zhou, Cenozoic sedimentation history of the central North Pacific: inferences from the elemental geochemistry of core LL44-GPC3, Geochim. Cosmochim. Acta 57 (1993) 1719–1740.
[7] S. Nakai, A.N. Halliday, D.K. Rea, Provenance of dust in the Pacific Ocean, Earth Planet. Sci. Lett. 119 (1993) 143–157.
[8] C.E. Jones, A.N. Halliday, D.K. Rea, R.M. Owen, Neodymium isotopic variations in North Pacific modern silicate sediment and the insignificance of detrital REE contributions to seawater, Earth Planet. Sci. Lett. 127 (1994) 55–56.
[9] C.E. Jones, A.N. Halliday, D.K. Rea, R.M. Owen, Eolian inputs of lead to the North Pacific, Geochim. Cosmochim. Acta 64 (2000) 1405–1416.
[10] Y. Asahara, T. Tanaka, H. Kamioka, A. Nishimura, Asian continental nature of $^{87}Sr/^{86}Sr$ ratios in north central Pacific sediments, Earth Planet. Sci. Lett. 133 (1995) 105–116.
[11] V. Monastra, L.A. Derry, O.A. Chadwick, Multiple sources of lead in soils from a Hawaiian chronosequence, Chem. Geol. 209 (2004) 215–231.
[12] S. Toyoda, T. Naruse, Eolian dust from Asian deserts to the Japanese islands since the last glacial maximum: the basis for the ESR method, Chikei 23 (2002) 811–820.
[13] T. Nakano, Y. Yokoo, M. Nishikawa, H. Koyanagi, Regional Sr–Nd isotopic ratios of soil minerals in northern China as Asian dust fingerprints, Atmos. Environ. 38 (2004) 3061–3067.
[14] Y. Yokoo, T. Nakano, M. Nishikawa, H. Quan, Mineralogical variation of Sr–Nd isotopic and elemental compositions in loess and desert sand from the central Loess Plateau in China as a provenance tracer of wet and dry deposition in the northwestern Pacific, Chem. Geol. 204 (2004) 45–62.
[15] T. Pettke, A.N. Halliday, C.M. Hall, D.K. Rea, Dust production and deposition in Asia and the north Pacific Ocean over the past 12 Myr, Earth Planet. Sci. Lett. 178 (2000) 397–413.
[16] L.M. Prueher, D.K. Rea, Tephrochronology of the Kamchatka–Kurile and Aleutian Arcs: evidence for volcanic episodicity, J. Volcanol. Geotherm. Res. 106 (2001) 67–84.
[17] L. Zhou, F.T. Kyte, Sedimentation history of the South Pacific pelagic clay province over the last 85 million years inferred from the geochemistry of Deep Sea Drilling Project hole 596, Paleoceanography 7 (4) (1992) 441–465.
[18] K. Hyeong, S.-H. Park, C.M. Yoo, H.-K. Kin, Mineralogical and geochemical compositions of the eolian dust from the northeast equatorial Pacific and their implications on paleolocation of the intertropical convergence zone, Paleoceanography 20 (2005), doi:10.1029/2004PA001053.
[19] T. Pettke, A.N. Halliday, D.K. Rea, Cenozoic evolution of Asian climate and sources of Pacific seawater Pb and Nd derived from eolian dust of sediment core LL44-GPC3, Paleoceanography 17 (2002) 3.1–3.13.
[20] M. Lyle, et al., Leg 199 summary, Proceedings of the Ocean Drilling Program Initial Reports, vol. 199, 2002, pp. 1–87.
[21] J.J. Griffen, E.D. Goldberg, Clay mineral distributions in the Pacific Ocean, in: M.N. Hill (Ed.), The Sea, The Earth Beneath the Sea, vol. 3, 1963, pp. 728–741.
[22] G. Ravizza, B. Peucker-Ehrenbrink, The marine $^{187}Os/^{188}Os$ record of the Eocene–Oligocene transition: the interplay of weathering and glaciation, Earth Planet. Sci. Lett. 210 (2003) 151–165.

[23] D.K. Rea, T.R. Janecek, Mass-accumulation rates of the non-authigenic inorganic crystalline (eolian) component of the deep-sea sediments from the western mid-Pacific mountains, deep sea drilling project site 463, Initial Reports of the Deep Sea Drilling Project, vol. LXII, 1981, pp. 653–659.
[24] P. Richard, N. Shimizu, C.J. Allegre, $^{143}Nd/^{146}Nd$, a natural tracer: an application to oceanic basalts, Earth Planet. Sci. Lett. 31 (1976) 269–278.
[25] M.K. Reuer, E.A. Boyle, B.C. Grant, Lead isotope analysis of marine carbonates and seawater by multiple collector ICP-MS, Chem. Geol. 200 (2003) 137–153.
[26] K.D. Collerson, B.S. Kamber, R. Schoenberg, Applications of accurate, high precision Pb isotope ratio measurement by multi-collector ICP-MS, Chem. Geol. 88 (2002) 65–83.
[27] W. Todt, R.A. Cliff, A. Hanser, A.W. Hofmann, Evaluation $^{202}Pb–^{205}Pb$ double spike for high-precision lead isotope analysis, Geophys. Monogr. 95 (1996) 429–437.
[28] J. Imbrie, T.H. Van Andel, Vector analysis of heavy-mineral data, Geol. Soc. Amer. Bull. 75 (1964) 1131–1156.
[29] M. Leinen, N. Pisias, An objective technique for determining end member compositions and for partitioning sediments according to their sources, Geochim. Cosmochim. Acta 48 (1983) 47–62.
[30] E. Weber, R.M. Owen, G.R. Dickens, A.N. Halliday, C.F. Jones, D.K. Rea, Quantitative resolution of eolian continental crustal material and volcanic detritus in North Pacific surface sediment, Paleoceanography 11 (1996) 115–127.
[31] J. Imbrie, N.G. Kipp, A new micropaleontology method for quantitative paleoclimatology: application to a late Pleistocene Caribbean core, Late Cenozoic Glacial Ages, Yale University Press, 1971, pp. 71–181.
[32] Richard Reyment, K.G. Joreskog, Applied Factor Analysis in the Natural Sciences, Cambridge University Press, 1993 371 pp.
[33] G. Faure, Isotope Geology, Wiley (1986) 589 pp.
[34] B. Jahn, S. Gallet, J. Han, Geochemistry of the Xining, Xifeng and Jixian sections, Loess Plateau of China: eolian dust provenance and paleosol evolution during the last 140 ka, Chem. Geol. 178 (2001) 71–94.
[35] Y. Asahara, $^{87}Sr/^{86}Sr$ variation in North Pacific sediments: a record of the Milankovitch cycle in the past 3 million years, Earth Planet. Sci. Lett. 171 (1999) 453–464.
[36] F.E. Grousset, M. Parra, A. Bory, P. Martinez, P. Bertrand, G. Shimmield, R.M. Ellan, Saharan wind regimes traced by the Sr–Nd isotopic composition of subtropical Atlantic sediments: last glacial maximum vs. today, Quat. Sci. Rev. 17 (1998) 395–409.
[37] A. Eisenhauer, H. Meyer, V. Rachold, T. Tutken, B. Wiegand, B. T. Hanser, R.F. Spielhagen, F. Lindemann, H. Kassens, Grain size separation and sediment mixing in Arctic Ocean sediments: evidence from the strontium isotope systematic, Chem. Geol. 158 (1999) 173–188.
[38] L.V. Godfrey, Temporal changes in the lead isotopic composition of red clays: comparison with ferromanganese crust records, Chem. Geol. 185 (2002) 241–254.
[39] J. Smith, D. Vance, R.A. Kemp, C. Archer, P. Toms, M. King, M. Zarate, Isotopic constraints on the source of Argentinian loess — with implications for atmospheric circulation and the provenance of Antarctic dust during recent glacial maxima, Earth Planet. Sci. Lett. 212 (2003) 181–196.
[40] D.K. Rea, S.A. Hovan, Grain size distribution and depositional processes of the mineral component of abyssal sediments: lessons from the North Pacific, Paleoceanography 10 (1995) 251–258.
[41] T. Van de Flierdt, M. Frank, A.N. Halliday, J.R. Hein, B. Hattendorf, D. Gunther, P.W. Kubik, Lead isotopes in North Pacific deep water — implications for past changes in input sources and circulation patterns, Earth Planet. Sci. Lett. 209 (2003) 149–164.
[42] Z.T. Guo, W.F. Ruddiman, Q.Z. Hao, H.B. Wu, Y.S. Qiao, R.X. Zhu, S.Z. Peng, J.J. Wei, B.Y. Yuan, T.S. Liu, Onset of Asian desertification by 22 Myr ago inferred from loess deposits in China, Nature 416 (2002) 159–163.
[43] S.M. McLennan, S.R. Taylor, M.T. McCulloch, J.B. Maynard, Geochemical and Nd–Sr isotopic composition of deep-sea turbidites: crustal evolution and plate tectonic associations, Geochim. Cosmochim. Acta 54 (1990) 2015–2050.
[44] S.R. Hemming, S.M. McLennan, Pb isotope compositions of modern deep sea turbidites, Earth Planet. Sci. Lett. 184 (2001) 489–503.
[45] Diepenbroek, M., Grobe, H., Sieger, R., 2000, PanMap, http://www.pangaea.de/Software/PanMap.
[46] M. Leinen, The origin of paleochemical signatures in North Pacific pelagic clays: partitioning experiments, Geochim. Cosmochim. Acta 51 (1987) 305–319.
[47] W.A. Berggren, D.V. Kent, C.C. Swisher, M.P. Aubrey, A revised Cenozoic geochronology and chronostratigraphy, in: W.A. Berggren, D.V. Kent, J. Hardenbol (Eds.), Geochronology and Global Stratigraphic Correlations: A Unified Temporal Framework for an Historical Geology. SEPM Special vol. 54, 1995, pp. 129–212.